*Journal of Ceramic Processing Research. Vol. 11, No. 6, pp. 769~772 (2010)*

J O U R N A L O F
**Ceramic Processing Research**

# Dependence of the structural and optical properties on the zinc nitrate concentration in ZnO nanowires formed on indium-tin-oxide-coated glass substrates

**Hee Yeon Yang and Tae Whan Kim***

*Department of Information Display Engineering, Department of Electronics and Communications Engineering, Hanyang University, Seoul 133-791, Korea*

**Scanning electron microscopy images showed that ZnO nanowires were formed on indium-tin-oxide-coated glass substrates by using an electrochemical deposition method and that the deposition efficiency of ZnO nanowires increased with increasing $Zn(NO_3)_2$ concentration. X-ray diffraction patterns showed that the ZnO nanowires had the Wurzite structure. Photoluminescence spectra at 300 K for ZnO nanowires formed with $Zn(NO_3)_2$ concentrations of 0.1, 0.5, and 1.0 mM showed that the full widths at half maximum of the near band-edge emission PL peak for ZnO nanowires formed with a $Zn(NO_3)_2$ concentration of 1.0 mM had the smallest value, indicative of the best crystalline quality. These results indicate that the structural and the optical properties of ZnO nanowires are improved by changing the $Zn(NO_3)_2$ concentration.**

**Key words: ZnO nanowire, structural property, optical property, electrochemical deposition, zinc nitride concentration.**

## Introduction

ZnO semiconductor materials have been currently receiving considerable attention due to their promising applications in memory devices [1], light-emitting diodes [2], photodetectors [3], lasers [4], solar cells [5], nanogenerators [6], and sensors [7] because they have wide energy gaps with unique physical properties of large exciton binding energies and excellent chemical stabilities [8]. The prospect of potential applications of electronic and optoelectronic devices fabricated utilizing ZnO nanostructures has led to substantial research and develpoment efforts to form the nanostructures by using various growth methods [9-12]. ZnO nanostructures have been extensively formed using physical vapor deposition (PVD) [9], chemical vapor deposition (CVD) [10], and pulsed laser deposition (PLD) [11]. Even though the ZnO nanostructures with a high quality have been grown by using PVD, CVD, and PLD methods, the formation methods require precise control of the vacuum and high temperature conditions. Therefore, an electrochemical deposition (ECD) method with a simple process has been used to grow large-area ZnO nanostructures at low temperature [13]. Although some studies concerning the formation and the physical properties of ZnO nanowires have been performed [14, 15], systematic studies on the dependence of the structural and optical properties on the zinc nitrate concentration in ZnO nanowires formed on indium-tin-oxide (ITO)-coated glass substrates grown by the ECD method are necessary to improve the device efficiency.

*Corresponding author:
Tel : +82-2-2220-0354
Fax: +82-2-2292-4153
E-mail: twk@hanyang.ac.kr

This paper reports the dependence of the structural and optical properties on the zinc nitrate concentration in ZnO nanowires formed on ITO-coated glass substrates by using the ECD method. Scanning electron microscopy (SEM) and X-ray diffraction (XRD) measurements were performed to characterize the structural properties of the ZnO nanowires formed. Photoluminescence (PL) measurements were performed to investigate the optical properties of the ZnO nanowires. The effect of the zinc nitrate concentration on the structural and the optical properties of ZnO nanowires formed on ITO-coated glass substrates was investigated.

## Experimental Details

ZnO nanowires used in this study were formed on ITO-coated glass substrates using ECD. The ZnO nanowires were formed resulting from the reduction of dissolved molecular oxygen in a zinc nitrate solution [16, 17]. The electrochemical reduction of oxygen molecules comes from the combination between the precursor and the current of the cathode [18, 19]. The diameter and the deposition efficiency of ZnO nanowires were controlled by using the growth conditions of ECD. ZnO nanowires with different diameters were grown by changing the mole density of the precursor and the current of the cathode. The ECD equipment for the growth of ZnO nanowires consists of three electrode electrochemical cells with an ITO cathode acting as a working electrode, a Pt electrode acting as a counter electrode, and a saturated calomel electrode (SCE) acting as a reference electrode. The $Zn(NO_3)_2$ and potassium chloride (0.1 M) were dissolved in a 200 ml deionized water. The KCl (SIGMA-ALDRICH, 99.0%-100.5%) acts as a supporting precursor [20]. The $Zn(NO_3)_2 \cdot 6H_2O$ (SIGMA-ALDRICH, 98.0%) acts as a $Zn^{2+}$ precursor. The

concentrations of $Zn(NO_3)_2$ solutions were 0.1, 0.5, and 1.0 mM. The resistivity of the ITO film was 17 Ω/square. The ZnO nanowires were electrochemically deposited at 70 °C under a constant applied voltage of −1.1 V for 4 h. The rapid thermal annealing process was performed in air at 400 °C for 2 minutes.

SEM measurements were performed using a scanning electron microscope (Quanta 50 Series, FEI Company), XRD measurements were carried out by a Rigaku D/MAX-2500 diffractometer with Cu $K_\alpha$ radiation, which was operated at a scanning rate of 5°/minute for a 2θ range between 20° and 65°. The photoluminescence measurements were carried out using a 50-cm monochromator equipped with an RCA 31034 photomultiplier tube. The excitation source was the 325-nm line of a He-Cd laser, and the sample temperature was kept at 300 K.

## Results and Discussion

Fig. 1 shows the SEM images of ZnO nanowires formed with different [$Zn(NO_3)_2$] concentrations. The applied voltage between the ITO and the SCE electrode was −1.1 V, and the concentration of the KCl solution was 0.1 M. The growth temperature and the growth time were 70 °C and 4 h, respectively. The diameter of the ZnO nanowires increases with increasing $Zn(NO_3)_2$ concentration due to an increase in the particle size at an initial formation stage resulting from the increase of the $Zn(NO_3)_2$ concentration [21, 22]. The density of the ZnO nanowires is varied by changing $Zn(NO_3)_2$ concentration.

Fig. 2 shows that the diameter and the deposition efficiency of the ZnO nanowires as functions of the $Zn(NO_3)_2$ concentration. The diameter and the deposition efficiency of ZnO nanowires increase with increasing current density between the ITO and the SCE electrodes due to an increase in the ratio between the $OH^-$ generation and the $Zn^{2+}$ diffusion with an increase in the mole density of the $Zn(NO_3)_2$. The existence of the Coulomb force between the ZnO nanowires and the cathode results in the out-of-plane growth of the ZnO nanowires with a vertical direction.

XRD patterns of the ZnO nanowires formed using different $Zn(NO_3)_2$ concentrations of 0.1, 0.5, and 1.0 mM are shown in Fig. 3. XRD patterns show that the ZnO nanowires have the Wurzite structure with cell parameters of a = 3.249 Å and c = 5.206 Å, which are in reasonable agreement with the literature values (JCPDS card, no. 36-1451). No XRD peak related to the $Zn(OH)_2$ appears in the XRD data, indicating that only single-phase ZnO nanowires are formed in the sample. The small value of the full widths at half maximum (FWHM) of the XRD peak corresponding to the ZnO nanowires indicates that the crystal quality of the synthesized ZnO nanowires is good.

When ZnO nanowires are grown with a low concentration of the $Zn(NO_3)_2$, because the density of the ZnO nanowire is relatively small, the diffraction intensity of the (0002) peak corresponding to the ZnO nanowires is smaller than those of the XRD peaks related to the ITO film, as shown

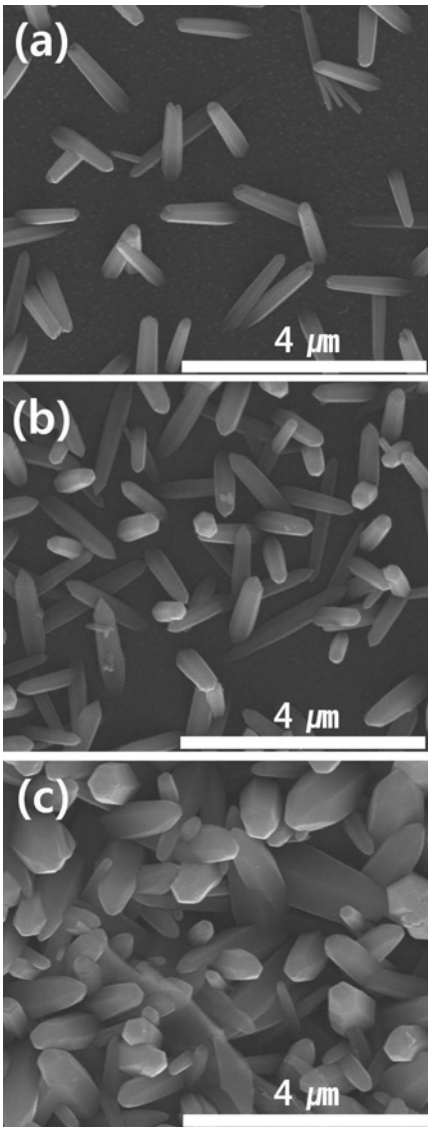


**Fig. 1.** Plane-view scanning electron microscopy images of the ZnO nanowires formed using $Zn(NO_3)_2$ concentrations of (a) 0.1, (b) 0.5, and (c) 1.0 mM.

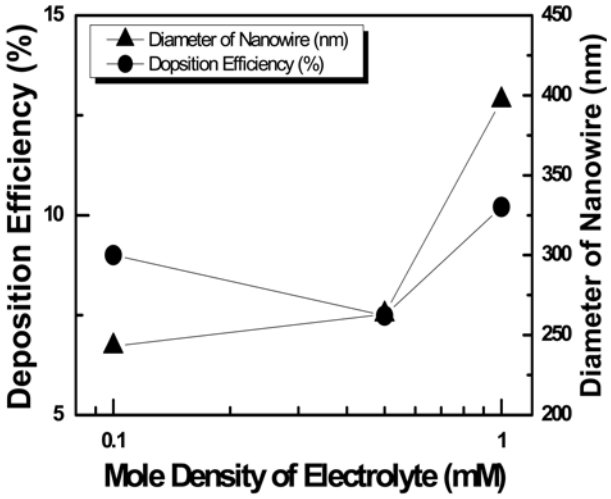


**Fig. 2.** Diameter and deposition efficiency as functions of the $Zn(NO_3)_2$ concentration for ZnO nanowires.

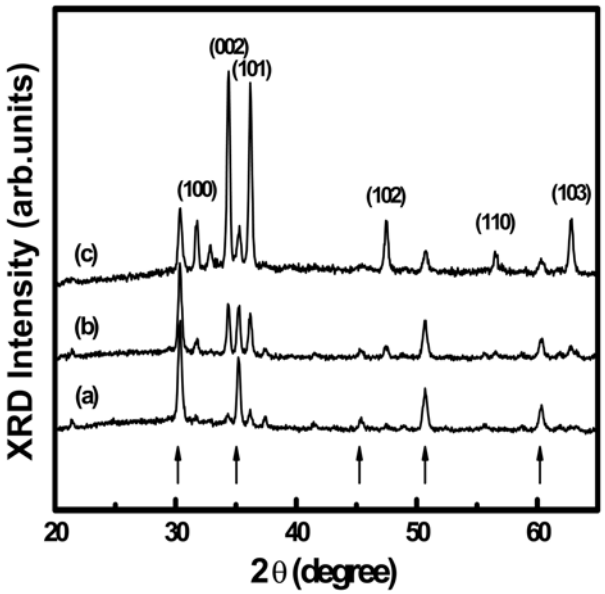


**Fig. 3.** X-ray diffraction (XRD) patterns of the ZnO nanowires formed using $Zn(NO_3)_2$ concentrations of (a) 0.1, (b) 0.5, and (c) 1.0 mM. The arrows indicate the XRD peaks related to the ITO film.

in Figs. 3(a) and 3(b). The diffraction intensity of the (0002) peak corresponding to the ZnO nanowires increases with increasing $Zn(NO_3)_2$ concentration, as shown in Fig. 3(c), indicating that ZnO nanowires are highly oriented with a c-axis perpendicular to the ITO-coated glass substrate. When the concentration of the $Zn(NO_3)_2$ is 1.0 mM, the intensities of (1000) and (0101) diffraction peaks corresponding to the ZnO nanowires shown in Fig. 3(c) slightly increases in comparison with those of ZnO nanowires shown in Figs. 3(a) and 3(b).

Fig. 4 shows the PL spectra at 300 K for the ZnO nanowires formed using different $Zn(NO_3)_2$ concentrations of 0.1, 0.5, and 1.0 mM. The emission peak appearing in the ultraviolet (UV) range is attributed to the direct recombination of the free excitons through an exciton-exciton collision process, which corresponds to the near band edge emission (NBE) [21]. NBE peaks with a small FWHM are observed at 382, 383 and 387 nm in the UV range, as shown Figs. 4(a), 4(b), and 4(c), respectively. Fig. 4(a) shows that the PL intensity of the dominant NBE peak for ZnO nanowires formed by a $Zn(NO_3)_2$ concentration of 0.1 mM is small due to the lower density of ZnO nanowires. The PL intensity corresponding to the NBE peak for ZnO nanowires increase with increasing $Zn(NO_3)_2$ concentration resulting from the increase in the ZnO density. The FWHM values of the NBE peak for ZnO nanowires formed with $Zn(NO_3)_2$ concentrations of 0.1, 0.5, and 1.0 mM are 24, 29, and 17 nm, respectively.

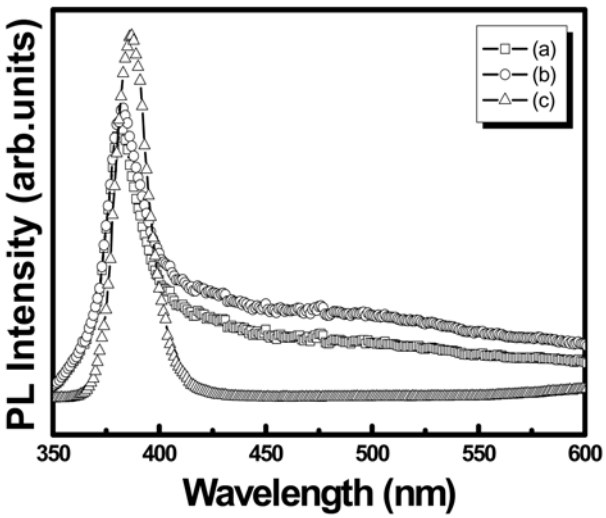


**Fig. 4.** Photoluminescence spectra at 300 K for ZnO nanowires formed using $Zn(NO_3)_2$ concentrations of (a) 0.1, (b) 0.5, and (c) 1.0 mM.

## Summary and Conclusions

The effect of the zinc nitrate concentration on the structural and the optical properties of ZnO nanowires formed on ITO-coated glass substrates using ECD was investigated. The structural and the optical properties of ZnO nanowires were varied by changing the concentration of the $Zn(NO_3)_2$ precursor. The deposition effieciency of ZnO nanowires was increased with increasing $Zn(NO_3)_2$ concentration. XRD patterns showed that the ZnO nanowires had the Wurzite structure with cell parameters of a = 3.249 Å and c = 5.206 Å. The FWHM values of the NBE peak of the PL spectra at 300 K for ZnO nanowires formed with $Zn(NO_3)_2$ concentrations of 0.1, 0.5, and 1.0 mM were 24, 29, and 17 nm, respectively. These results indicate that the structural and the optical properties of the ZnO nanowires formed using ECD was very good. Furthermore, the present observations can help to improve an understanding of the effect of the zinc nitrate concentration on the structural and the optical properties of ZnO nanowires.

## Acknowledgements

This work was supported by the National Research Foundation of Korea (NRF) grant funded by the Korea government (MEST) (No. 2010-0018877).

## References

1. F. Li, D.I. Son, S.H. Cho and T.W. Kim, Nanotechnology 20 (2009) 185202-1-185202-4.
2. P.A. Savariumuthu, I.L. Jeong and K.K. Jin, Appl. Phys. Lett. 90 (2007) 103107-1-103107-3.
3. C. Soci, C. Zhang, B. Xiang, S.A. Dayeh, D.P.R. Aplin, J. Park, X.Y. Bao, Y.H. Lo and D. Wang, Nano Lett. 7 (2007) 1003-1009.
4. H. Zhu, C.X. Shan, B. Yao, B.H. Li, J.Y. Zhang, Z.Z. Zhang, D.X. Zhao, D.Z. Shen, X.W. Fan, Y.M. Lu and Z.K. Tang, Adv. Mater. 21 (2009) 1613-1617.
5. T. Atsushi, O. Akira, O. Takeyoshi, O. Makoto, M. Takayuki, M. Sumiya, K. Ohtani, S.F. Chichibu, S. Fuke, Y. Segawa, H. Ohno, H. Koinuma and M. Kawasaki, Nat. Mater. 4 (2005) 42-46.

6. M-P. Lu, J. Song, M-Y. Lu, M-T. Chen, Y. Gao, L-J. Chen and Z.L. Wang, Nano Lett. 9 (2009) 1223-1227.
7. J. Zhou, Y. Gu, P. Fei, W. Mai, Y. Gao, R. Yang, G. Bao and Z.L. Wang, Nano Lett. 8 (2008) 3035-3040.
8. C.C. Li, Z.F. Du and L.M. Li, Appl. Phys. Lett. 91 (2007) 032101-1-032101-3.
9. L.C. Campos, S.H. Dalal, D.L. Baptista, R. Magalhães-Paniago, A.S. Ferlauto, W.I. Milne, L.O. Ladeira and R.G. Lacerda, Appl. Phys. Lett. 90 (2007) 181929-1-181929-3.
10. G.D. Yuan, W.J. Zhang, J.S. Jie, X. Fan, J.A. Zapien, Y.H. Leung, L.B. Luo, P.F. Wang, C.S. Lee and S.T. Lee, Nano Lett. 8 (2008) 2591-2597.
11. J. Zuniga-Perez, A. Rahm, C. Czekalla, J. Lenzner, M. Lorenz and M. Grundmann, Nanotechnology 18 (2007) 195303-1-195303-7.
12. Z.L. Wang, Mater. Sci. Eng. R-Rep. 64 (2009) 33-77.
13. J.S. Wellings, N.B. Chaure, S.N. Heavens and I.M. Dharmadasa, Thin Solid Films 516 (2008) 3893-3898.
14. B. Xiang, P. Wang, X. Zhana, S.A. Dayeh, D.P.R. Aplin, C. Soci, D. Yu and D. Wang, Nano Lett. 7 (2007) 323-328.
15. R. Tena-Zaera, J. Elias, C. Lévy-Clément, C. Bekeny, T. Voss, I. Mora-Seró and J. Bisquert, J. Phys. Chem. C 112 (2008) 16318-16323.
16. S. Peulon and D. Lincot, Adv. Mater. 8 (1996) 166-170.
17. R. Konekamp, K. Boedecker, M.C. Lus-Steiner, M. Poschenrieder, F. Zenia, C. Levy-Clement and S. Wangner, Appl. Phys. Lett. 77 (2000) 2575-2577.
18. S. Strbac and R.R. Adzic, Electrochim. Acta 41 (1996) 2903-2908.
19. S.P. Jiang, C.Q. Cui and A.C.C. Tseung, J. Electrochem. Soc. 138 (1992) 3599-3605.
20. R. Tena-Zaera, J. Elias, G. Wang and C. Levy-Clement, J. Phys. Chem. C 111 (2007) 16706-16711.
21. A. Umar and Y.B. Hahn, Nanotechnology 17 (2006) 2174-2180.
22. C. Burda, X. Chen, R. Narayanan and M. A. El-Sayed, Chem. Rev. 105 (2005) 1025-1102.